Journal of Achievements in Materials and Manufacturing Engineering

VOLUME 55
ISSUE 1
November
2012

A study on simulation model and kinematic model of welding robot

J.W. Jeong, I.S. Kim*, R.R. Chand, J.H. Lee
Department of Mechanical Engineering, Mokpo National University,
16, Dorim-ri, Chungkye-myun, Muan-gun, Jeonnam 534-729, South Korea
* Corresponding e-mail address: ilsookim@mokpo.ac.kr

Received 12.09.2012; published in revised form 01.11.2012

Analysis and modelling

ABSTRACT

Purpose: This study tries to develop a simulation model of six degree freedom for Faraman AM1 welding robot using CATIA V5 and compares with the computed kinematic model for robotic welding. The error varification of simulated model and kinematics of the robot is also being carried out.

Design/methodology/approach: CATIA (Computer Aided Three dimensional Interactive Application) is a multi-platform PLM/CAD/CAM/CAE commercial software suite to use to develop six degree freedom for Faraman AM1 welding robot. The forward kinematic and inverse kinematic equations are also used to verify the developed model.

Findings: The results obtained from the six degree freedom for Faraman AM1 simulated model has a good agreement with computed kinematic models equations. The catia V5 a very powerful tool which could used in develope a simulation for robotic welding system. The the angle error between simulated model and computed inverse kinmenatic equation obtained too very small.

Research limitations/implications: The developed simulated in Catia is mainly aimed to be used in GMA welding process. D-H (Denavit-Hartenberg) convection is used to determine the orthonormal coordinate frames at different joints of a robotic manipulator and determining four kinematic parameters.

Originality/value: The six degree freedom for Faraman AM1 welding robot is model to analysed and compared with forward and inverse knimatic.

Keywords: CATIA V5; Simulation model; Faraman AM; Forward kinematic; Inverse kinematic; Denavit-Hartenburg parameters; Welding robots

Reference to this paper should be given in the following way:
J.W. Jeong, I.S. Kim, R.R. Chand, J.H. Lee, A study on simulation model and kinematic model of welding robot, Journal of Achievements in Materials and Manufacturing Engineering 55/1 (2012) 66-73.

1. Introduction

Robotics welding has been one of the main automatic welding tasks for complex products in manufacturing industry. Measurement of welding-induced deformation is normally performed to provide the dimensions of the welded structure during or after the welding and in some case it was used to provide the actual data for examining the accuracy of the mathematical, numerical or empirical prediction. To archive the high quality as well as to save time and reduce cost of welding systems, the simulation of welding system need to be developed. Simulation allows researchers, designer and user verify the collisions between the torch and weld product, optimized the motion sequence of welding robot. It can also be a powerful tool to estimate and predict the welding heat effects before the real welding products process begin.

Research on simulation model of GMA robotic welding system and kinematic model is not novel, but many efforts have been carried out to develop for various simulation models of welding systems. Cheng [3] introduced a methodology for developing required robotic workcell simulation models via Deneb IGRIP robotic simulation technology. Ericsson et al. [4] presented a system that combines robot off-line programming software with a finite element model that predicts temperature-time histories and residual stress distributions. Pashkevich et al. [5] focused on the kinematic control of a robotic system which consists of a 6-axis industrial robot and a 2-axis welding positioner that is intended to optimize a weld joint orientation relative to the gravity during the technological process. Ang Jr. et al. [6] developed a system namely SWERS for the welding process. The main feature SWERS is the walk-through (or direct teaching) method for robot programming. The welder teaches the robot by guiding it once through the required welding motions, the motion is recorded and the robot thereafter does the unpleasant job of welding by "playing back" the recorded motions. Optimized welding parameters can be selected from a large database though a Graphical User Interface system.In aother case, Tung et al. [7] developed a mobile robotic system as a substitute for manual SMA welding repair processes. Two installed in parallel CCD cameras were used to initially detect the position of a crack and then used to drive the robot at a constant welding speed along the desired welding path. A new algorithm for processing the binocular images and obtaining the crack positions was proposed and the equations for the forward and inverse kinematics of five-axis SCORBOT-ER VII robot also been derived.

Robot kinematics is the study of the motion (kinematics) of robots. In a kinematic analysis for the position, the velocity and the acceleration of all the links are calculated without considering the forces that cause this motion. Robot kinematics deals with aspects of redundancy, collision avoidance and singularity avoidance. While dealing with the kinematics used in the robots each parts of the robot by assigning a frame of reference to it should be analyzed and hence a robot with many parts may have many individual frames assigned to each movable parts. For simplicity the single manipulator arm of the robot should be considered. Each frame are named systematically with numbers, for example the immovable base part of the manipulator is numbered 0, and the first link joined to the base is numbered 1, and the next link 2 and similarly till for the last *th* link.

CATIA (Computer Aided Three dimensional Interactive Application) is a multi-platform PLM/CAD/CAM/CAE commercial software suite developed by Dassault Systemes and marketed world-wide by IBM. CATIA V5 is the leading product development solution for all manufacturing organizations. Lin et al. [8] developed an automated design system for drawing dies. This die design system is built on top of CATIA V5, and makes use of its built-in modules, including 12 Part Design, Automation and Scripting, and Knowledge Advisor. Skarka [9] employed MOKA methodology and in particular its informal knowledge model and knowledge representation for generative model, which is special for CATIA. Chu et al. [10] developed a computer aided parametric design system for 3D tire mold production. The 3D mold was modeled with the GSM module. A customized mold creation module has been developed using CAA to demonstrate the feasibility of the design framework. The proposed geometric algorithms were also implemented with C++ CAA and other programming resources (GUI's, memory management tools, and graphics) provided by the software.

This paper tried to develop and validate a simulation model of six degree freedom for Faraman AM1 welding robot using CATIA V5. CATIA software was chosen because of it has a lot of powerful tools for developing a simulation one. To varify the error associate with simulation model and as well as the error associated with the kinematics of the robot. Digital Mockup workbench of CATIA has a module known as DMU Kinematics where the former type of dynamic solutions can be perform. CATIA's Knowledgeware modules allow expand the automation of welding process by using some different kind of intrinsic knowledge forms such as: parameters, formulas, design table, rules and checks.And with the use of additional functionality such as Visual Basic CAA V5 or C++ CAA V5, the extra program can be developed for better fit with the customer requirements.

2. Kinematics

In the kinematic analysis of manipulator position, there are two separate problems to solve such as forward kinematics, and inverse kinematics. Forward kinematics involves solving the forward transformation equation to find the location of the hand in terms of the angles and displacements between the links. Inverse kinematics is the more difficult problem to solve and, for some manipulators, closed form solutions cannot be found. However, constraints are usually placed on manipulator design so that the inverse solution can be found; without this, the robot is difficult to control in Cartesian space. For this study the D-H (Denavit-Hartenberg) convention is used.

2.1. D-H (Denavit-Hartenberg) convention

D-H notation is a universal method for assigning right handed orthonormal coordinate frames to the different joints of a robotic manipulator and determining four kinematic parameters, which relate to specific aspects of the spatial relationship between links i-1 and i, to build a complete link transformation matrix between coordinate frame i-1 and coordinate frame i.

In Fig. 1, link i connects link $i - 1$ to link $i + 1$ through a_i. The figure is used to demonstrate the steps involved in determining the Denavit and Hartenberg parameters.

The following steps denote the systematic derivation of the D-H parameters [11].

1. Label each axis in the manipulator with a number starting from 1 as the base to n_A as the end effector. O_o is the origin of the base coordinate frame. Every joint must have an axis assigned to it.
2. Set up a coordinate frame for each joint. Starting with the base joint, set up a right handed coordinate frame for each joint. For a rotational joint, the axis of rotation for axis i is always along Z_{i-1}. If the joint is a prismatic joint, Z_{i-1} should point in the direction of translation.
3. The X_i axis should always point away from the Z_{i-1} axis.
4. Y_i should be directed such that a right-handed orthonormal coordinate frame is created.
5. For the next joint, if it is not the end effector frame, steps 2–4 should be repeated.

6. For the end effector, the Z_{nA} axis should point in the direction of the end effector approach.
7. θ_i is the rotation about Z_{i-1} to make X_{i-1} parallel to X_i (going from X_{i-1} to X_i).
8. α_i is the rotation about X_i axis to make Z_{i-1} parallel to Z_i (going from Z_{i-1} to Z_i).
9. a_i is the perpendicular distance between axis i and axis i + 1.
10. d_i is the offset along the Z_{i-1} axis as shown schematically in Fig. 1. Thus d_i is the distance between O_{i-1} and O_i along Z_{i-1} (axis i).

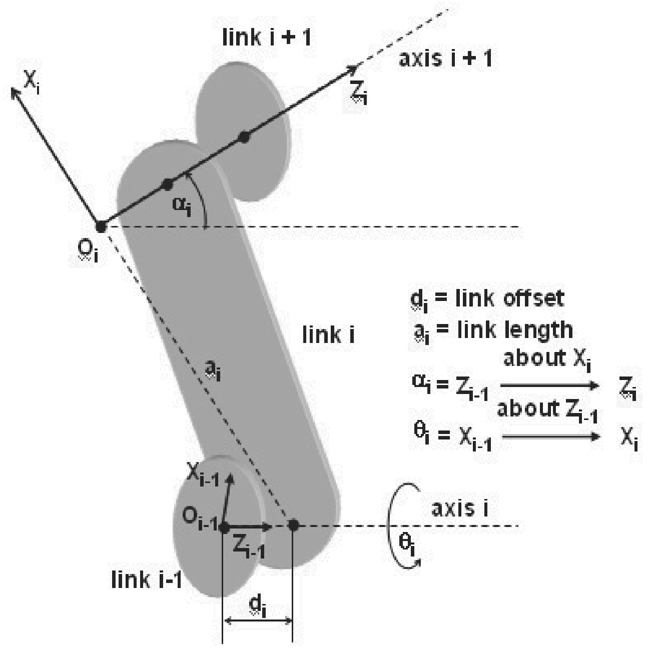

Fig. 1. Schematic for determining the Denavit-Hartenburg parameters [11]

In general, four elementary transformations are required to relate the i-th coordinate frame to the (i-1)-th coordinate frame;

$$\mathbf{T}_{i-1}^{i} = \mathrm{Rot}\,(Z,\theta_i)\ \mathrm{Trans}\,(Z,d_i)\ \mathrm{Trans}\,(X,a_i)\ \mathrm{Rot}\,(X,\alpha_i)$$

where:

- θ_i, d_i, a_i, α_i are four kinematic parameters. Parameters a_i and α_i are constant values and are based on the geometry of the manipulator, while parameters d_i and θ_i can be variable that depend on whether the joint is prismatic or revolute.
- Rot (Z, θ_i): Rotate about the Z_{i-1} axis in the right-handed sense an angle of θ_i to make the X_{i-1} axis parallel to X_i axis
- Trans (Z, d_i): Translate along the positive direction of the Z_{i-1} axis a distance of d_i to make the X_{i-1} axis and X_i axis collinear.
- Trans (X, a_i): Translate along the positive direction of $X_{i-1}=X_i$ axis a distance of a_i to bring the origin O_{i-1} to O_i.
- Rot (X, α_i): Rotate about the $X_{i-1}=X_i$ axis in the right-handed sense an angle of α_i to coalesce the two coordinate frames.

So, the link transformation matrix between coordinate frame i-1 and coordinate frame i has the following form;

$$\mathbf{T}_{i-1}^{i} = \begin{bmatrix} \cos\,\theta_i & -\sin\,\theta_i & 0 & 0 \\ \sin\,\theta_i & \cos\,\theta_i & 0 & 0 \\ 0 & 0 & 1 & 0 \\ 0 & 0 & 0 & 1 \end{bmatrix} \begin{bmatrix} 1 & 0 & 0 & 0 \\ 0 & 1 & 0 & 0 \\ 0 & 0 & 1 & d_i \\ 0 & 0 & 0 & 1 \end{bmatrix}$$
$$\begin{bmatrix} 1 & 0 & 0 & a_i \\ 0 & 1 & 0 & 0 \\ 0 & 0 & 1 & 0 \\ 0 & 0 & 0 & 1 \end{bmatrix} \begin{bmatrix} 1 & 0 & 0 & 0 \\ 0 & \cos\,\alpha_i & -\sin\,\alpha_i & 0 \\ 0 & \sin\,\alpha_i & \cos\,\alpha_i & 0 \\ 0 & 0 & 0 & 1 \end{bmatrix}$$

$$\mathbf{T}_{i-1}^{i} = \begin{bmatrix} \cos\theta_i & -\sin\theta_i\cos\alpha_i & \sin\theta_i\sin\alpha_i & a_i\cos\theta_i \\ \sin\theta_i & \cos\theta_i\cos\alpha_i & -\cos\theta_i\sin\alpha_i & a_i\sin\theta_i \\ 0 & \sin\alpha_i & \cos\alpha_i & d_i \\ 0 & 0 & 0 & 1 \end{bmatrix}$$

2.2. Forward kinematics

Fig. 2 is the six degrees of freedom Faraman AM1 robot studied in this paper. Applying the D-H algorithm, the joint-coordinate diagram was archived as show in Fig. 3. The robot kinematics parameters such as joint angle, θ, joint distance, d, link length, a, and link twist angle, α, are presented in Table 1.

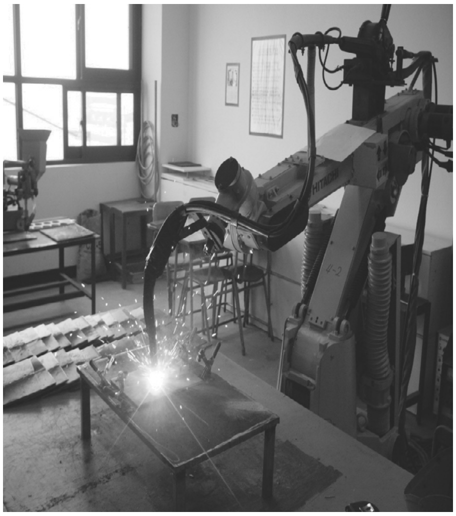

Fig. 2. Faraman AM1 welding robot

Table 1.
Kinematics parameters of Faraman M1 robot

Axis	θ	d (mm)	a (mm)	α
1	θ_1	0	$a_1 = 200$	$-\pi/2$
2	θ_2	0	$a_2 = 600$	0
3	θ_3	0	$a_3 = 135$	$-\pi/2$
4	θ_4	$d_4 = 750$	0	$\pi/2$
5	θ_5	0	0	$-\pi/2$
6	θ_6	0	0	0

Then, the link transformation matrix between coordinate frame 0 and coordinate frame 1 can be archived as shown below and others are the same:

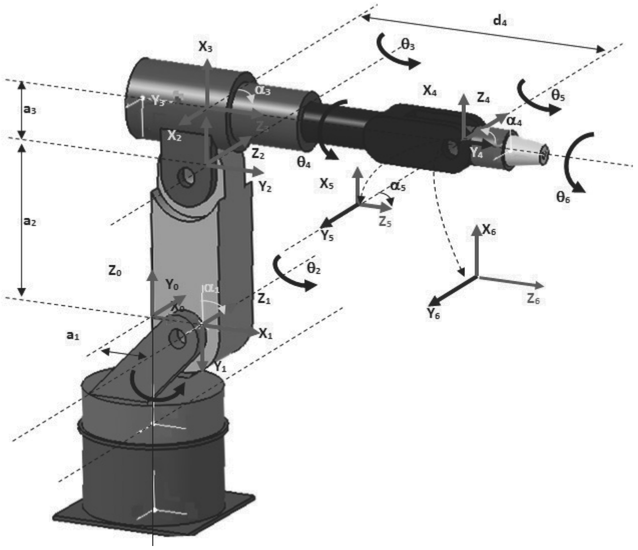

Fig. 3. Joint-coordinate diagram

$$T_0^1=\begin{bmatrix} C_1 & 0 & -S_1 & a_1C_1 \\ S_1 & 0 & C_1 & a_1S_1 \\ 0 & -1 & 0 & 0 \\ 0 & 0 & 0 & 1 \end{bmatrix} \quad T_1^2=\begin{bmatrix} C_2 & -S_2 & 0 & a_2C_2 \\ S_2 & C_2 & 0 & a_2S_2 \\ 0 & 0 & 1 & 0 \\ 0 & 0 & 0 & 1 \end{bmatrix}$$

$$T_2^3=\begin{bmatrix} C_3 & 0 & -S_3 & a_3C_3 \\ S_3 & 0 & C_3 & a_3S_3 \\ 0 & -1 & 0 & 0 \\ 0 & 0 & 0 & 1 \end{bmatrix} \quad T_3^4=\begin{bmatrix} C_4 & 0 & S_4 & 0 \\ S_4 & 0 & -C_4 & 0 \\ 0 & 1 & 0 & d4 \\ 0 & 0 & 0 & 1 \end{bmatrix}$$

$$T_4^5=\begin{bmatrix} C_5 & 0 & -S_5 & 0 \\ S_5 & 0 & C_5 & 0 \\ 0 & -1 & 0 & 0 \\ 0 & 0 & 0 & 1 \end{bmatrix} \quad T_5^6=\begin{bmatrix} C_6 & -S_6 & 0 & 0 \\ S_6 & C_6 & 0 & 0 \\ 0 & 0 & 1 & 0 \\ 0 & 0 & 0 & 1 \end{bmatrix}$$

Therefore the transformation matrix between tool frame and the base frame is obtained as follow:

$$T_0^6 = T_0^1T_1^2T_2^3T_3^4T_4^5T_5^6$$

$$T_0^6=\begin{bmatrix} r_{11} & r_{12} & r_{13} & p_x \\ r_{21} & r_{22} & r_{23} & p_y \\ r_{31} & r_{32} & r_{33} & p_z \\ 0 & 0 & 0 & 1 \end{bmatrix}$$

$$r_{11}=C_1(C_{23}C_4C_5C_6-S_{23}S_5C_6-C_{23}S_4S_6)+S_1(S_4C_5C_6+C_4S_6)$$

$$r_{21}=S_1(C_{23}C_4C_5C_6-S_{23}S_5C_6-C_{23}S_4S_6)-C_1(S_4C_5C_6+C_4S_6)$$

$$r_{31}=-S_{23}C_4C_5C_6-C_{23}S_5C_6+S_{23}S_4S_6$$

$$r_{12}=-C_1(C_{23}C_4C_5S_6-S_{23}S_5S_6+C_{23}S_4C_6)-S_1(S_4C_5S_6-C_4C_6)$$

$$r_{22}=-S_1(C_{23}C_4C_5S_6-S_{23}S_5S_6+C_{23}S_4C_6)+C_1(S_4C_5S_6-C_4C_6)$$

$$r_{32}=(S_{23}C_4C_5S_6+C_{23}S_5S_6+S_{23}S_4C_6)$$

$$r_{13}=-C_1(C_{23}C_4S_5+S_{23}C_5)-S_1S_4S_5$$

$$r_{23}=-S_1(C_{23}C_4S_5+S_{23}C_5)+C_1S_4S_5$$

$$r_{33}=S_{23}C_4S_5-C_{23}C_5$$

$$p_x=C_1(a_3C_{23}+a_2C_2+a_1-d_4S_{23})$$

$$p_y=S_1(a_3C_{23}+a_2C_2+a_1-d_4S_{23})$$

$$p_z=-a_3S_{23}-a_2S_2-d_4C_{23}$$

where:
$C_i=\cos(\theta_i);S_i=\sin(\theta_i);C_{23}=\cos(\theta_2+\theta_3);S_{23}=\sin(\theta_2+\theta_3)\quad(i=1..6)$

With a set of joint angles and position coordinate values from excel simulation output file, the forward kinematics can be easy to check.

2.3. Inverse kinematics

To solve for θ_1, consider the following equation:

$$(T_0^1)^{-1}T_0^6=(T_0^1)^{-1}T_0^1T_1^2T_2^3T_3^4T_4^5T_5^6=T_1^6$$

$$\begin{bmatrix} C_1 & S_1 & 0 & -a_1 \\ 0 & 0 & -1 & 0 \\ -S_1 & C_1 & 0 & 0 \\ 0 & 0 & 0 & 1 \end{bmatrix}\begin{bmatrix} r_{11} & r_{12} & r_{13} & p_x \\ r_{21} & r_{22} & r_{23} & p_y \\ r_{31} & r_{32} & r_{33} & p_z \\ 0 & 0 & 0 & 1 \end{bmatrix}=\mathbf{T}_1^6 \tag{2}$$

where;

$$\mathbf{T}_1^6=\begin{bmatrix} R'_{11} & R'_{12} & R'_{13} & P'_x \\ R'_{21} & R'_{22} & R'_{23} & P'_y \\ R'_{31} & R'_{32} & R'_{33} & P'_z \\ 0 & 0 & 0 & 1 \end{bmatrix}$$

$$R'_{11}=C_2[C_3(C_4C_5C_6-S_4S_6)-S_3S_5C_6]-S_2[S_3(C_4C_5C_6-S_4S_6)+C_3S_5C_6]$$

$$R'_{21}=S_2[C_3(C_4C_5C_6-S_4S_6)-S_3S_5C_6]+C_2[S_3(C_4C_5C_6-S_4S_6)+C_3S_5C_6]$$

$$R'_{31}=-(S_4C_5C_6+C_4C_6)$$

$$R'_{12}=C_2[C_3(-C_4C_5S_6-S_4C_6)+S_3S_5S_6]-S_2[S_3(-C_4C_5S_6-S_4C_6)-C_3S_5S_6]$$

$$R'_{22}=S_2[C_3(-C_4C_5S_6-S_4C_6)+S_3S_5S_6]-C_2[S_3(-C_4C_5S_6-S_4C_6)-C_3S_5S_6]$$

$$R'_{32}=-(-S_4C_5S_6+C_4C_6)$$

$$R'_{13}=C_2(-C_3C_4S_5-S_3C_5)-S_2(-S_3C_4S_5+C_3C_5)$$

$$R'_{23}=S_2(-C_3C_4S_5-S_3C_5)+C_2(-S_3C_4S_5+C_3C_5)$$

$$R'_{33}=S_4S_5$$

$$P'_x=C_2(-d_4S_3+a_3C_3)-S_2(d_4C_3+a_3S_3)+a_2C_2$$

$$P'_y=S_2(-d_4S_3+a_3C_3)+C_2(d_4C_3+a_3S_3)+a_2S_2$$

$$P'_z=0$$

To solve for θ_3, Equation the (3, 4) elements from both sides of the equation (2) have:

$$-S_1p_x+C_1p_y=0 \quad (\mathbf{T}_1^6(3,4)=0)$$

To solve above equation, the trigonometric substitution was made:

$$p_x=R\cos(\phi);\quad p_y=R\sin(\phi)\quad \text{where}\quad \phi=A\tan 2(p_y,p_x);\quad R=\sqrt{p_x^2+p_y^2}$$

Substituting yields:

$\sin(\phi-\theta_1)=0$. Hence $\cos(\phi-\theta_1)=\pm 1$

Therefore: $\phi-\theta_1=A\tan 2(0,\pm 1)$ (3)

That mean: $\theta_1=A\tan 2(p_y,p_x)-A\tan 2(0,\pm 1)$

Equation the (1, 4), (2, 4), (3, 4) elements from both sides of the equation (2) have:

$$C_1p_x+S_1p_y-a_1=C_2(-d_4S_3+a_3C_3)-S_2(d_4C_3+a_3S_3)+a_2C_2$$

$$-p_z=S_2(-d_4S_3+a_3C_3)+C_2(d_4C_3+a_3S_3)+a_2S_2$$

$$-S_1p_x+C_1p_y=0$$

Square these equations and add the resulting equations have:

$$2a_2(-d_4S_3+a_3C_3)=p_x^2+p_y^2+p_z^2-2a_1(p_xC_1+p_yS_1)-d_4^2-a_3^2-a_2^2+a_1^2$$

Let put:

$$K=\frac{p_x^2+p_y^2+p_z^2-2a_1(p_xC_1+p_yS_1)-d_4^2-a_3^2-a_2^2+a_1^2}{2a_2}$$

Therefore, have: $-d_4S_3+a_3C_3=K$

Once again, trigonometric substitution was used to yield result of θ_3

$$\theta_3=A\tan 2(a_3,d_4)-A\tan 2(K,\pm\sqrt{a_3^2+d_4^2-K^2}) \tag{4}$$

$$(T_0^3)^{-1}T_0^6=(T_2^3)^{-1}(T_1^2)^{-1}(T_0^1)^{-1}T_0^1T_1^2T_2^3T_3^4T_4^5T_5^6=T_3^6$$

$$\begin{bmatrix} C_1C_{23} & S_1C_{23} & -S_{23} & -a_1C_{23}-a_2C_3-a_3 \\ S_1 & -C_1 & 0 & 0 \\ -C_1S_{23} & -S_1S_{23} & -C_{23} & a_1S_{23}+a_2S_3 \\ 0 & 0 & 0 & 1 \end{bmatrix}\begin{bmatrix} r_{11} & r_{12} & r_{13} & p_x \\ r_{21} & r_{22} & r_{23} & p_y \\ r_{31} & r_{32} & r_{33} & p_z \\ 0 & 0 & 0 & 1 \end{bmatrix}=\mathbf{T}_3^6$$

Equation the (1, 4), (3, 4) elements from both sides of the equation (5) have:

$$C_1C_{23}p_x+S_1C_{23}p_y-S_{23}p_z-a_1C_{23}-a_2C_3-a_3=0$$

$$-C_1S_{23}p_x-S_1S_{23}p_y-C_{23}p_z+a_1S_{23}+a_2S_3=d_4$$

From these equations, C_{23} and S_{23} can be solved for:

$$S_{23}=\frac{-(a_2C_3+a_3)p_z+(a_2S_3-d_4)(C_1p_x+S_1p_y-a_1)}{(C_1p_x+S_1p_y-a_1)^2+p_z^2};$$

$$C_{23}=\frac{(a_2S_3-d_4)p_z+(a_2C_3+a_3)(C_1p_x+S_1p_y-a_1)}{(C_1p_x+S_1p_y-a_1)^2+p_z^2}$$

$$\theta_{23}=\theta_2+\theta_3=A\tan 2[-(a_2C_3+a_3)p_z+(a_2S_3-d_4)(C_1p_x+S_1p_y-a_1),\\ (a_2S_3-d_4)p_z+(a_2C_3+a_3)(C_1p_x+S_1p_y-a_1)]$$

With two solutions of θ_1 and two solutions of θ_3, four possible solutions for θ_2 are computed as:

$$\theta_2=\theta_{23}-\theta_3 \tag{6}$$

Equation the (1, 3), (2, 3) elements from both sides of the equation (5) have:

$$C_1C_{23}r_{13}+S_1C_{23}r_{23}-S_{23}r_{33}=-C_4S_5$$

$$S_1r_{13}-C_1r_{23}=-S_4S_5$$

If $S_5\neq 0$, θ_4 can be solved by:

$$\theta_4=A\tan 2[-(S_1r_{13}-C_1r_{23}),-(C_1C_{23}r_{13}+S_1C_{23}r_{23}-S_{23}r_{33})] \tag{7}$$

When $S_5=0$, joint axis 4 and 6 line up and cause the same motion of the link 6 of the robot. This situation can be detected by checking whether both argument of Atan2 are near zero. In this case θ_4 is usually chosen to be equal to the present value of θ_4 [14].

$$(T_0^4)^{-1}T_0^6=(T_3^4)^{-1}(T_2^3)^{-1}(T_1^2)^{-1}(T_0^1)^{-1}T_0^1T_1^2T_2^3T_3^4T_4^5T_5^6=T_4^6$$

$$(\mathbf{T}_0^4)^{-1}\begin{bmatrix} r_{11} & r_{12} & r_{13} & p_x \\ r_{21} & r_{22} & r_{23} & p_y \\ r_{31} & r_{32} & r_{33} & p_z \\ 0 & 0 & 0 & 1 \end{bmatrix}=\begin{bmatrix} C_5C_6 & -C_5S_6 & -S_5 & 0 \\ S_5C_6 & -S_5S_6 & C_5 & 0 \\ -S_6 & -C_6 & 0 & 0 \\ 0 & 0 & 0 & 1 \end{bmatrix} \tag{8}$$

Equation the (1, 3), (2, 3) elements from both sides of the equation (8) have:

$$-(C_4C_1C_{23}+S_4S_1)r_{13}-(C_4S_1C_{23}-S_4C_1)r_{23}+C_4S_{23}r_{33}=S_5$$

$$-C_1S_{23}r_{13}-S_1S_{23}r_{23}-C_{23}r_{33}=C_5 \qquad (9)$$

$$\theta_5 = A\tan 2[-(C_4C_1C_{23}+S_4S_1)r_{13}-(C_4S_1C_{23}-S_4C_1)r_{23} + C_4S_{23}r_{33}, (-C_1S_{23}r_{13}-S_1S_{23}r_{23}-C_{23}r_{33})]$$

$$(T_0^5)^{-1}T_0^6=(T_4^5)^{-1}(T_3^4)^{-1}(T_2^3)^{-1}(T_1^2)^{-1}(T_0^1)^{-1}T_0^1T_1^2T_2^3T_3^4T_4^5T_5^6=T_5^6$$

$$(\mathbf{T}_0^5)^{-1}\begin{bmatrix} r_{11} & r_{12} & r_{13} & p_x \\ r_{21} & r_{22} & r_{23} & p_y \\ r_{31} & r_{32} & r_{33} & p_z \\ 0 & 0 & 0 & 1 \end{bmatrix} = \begin{bmatrix} C_6 & -S_6 & 0 & 0 \\ S_6 & C_6 & 0 & 0 \\ 0 & 0 & 1 & 0 \\ 0 & 0 & 0 & 1 \end{bmatrix} \qquad (10)$$

Equation the (1, 1), (2, 1) elements from both sides of the equation (10) have:

$$[C_5(C_4C_1C_{23}+S_4S_1)-S_5C_1S_{23}]r_{11}+[C_5(C_4S_1C_{23}-S_4C_1)-S_5S_1S_{23}]r_{21} +[-C_5C_4S_{23}-S_5C_{23}]r_{31}=C_6$$

$$[-S_4C_1C_{23}+C_4S_1]r_{11}+[-S_4S_1C_{23}-C_4C_1]r_{21}+S_4S_{23}r_{31}=S_6$$

$$\theta_6 = A\tan 2(S_6, C_6)$$

3. Build the simulation model

The following steps were implemented to archive the simulation model:

- Model the 6 CATIA parts of the robot
- Create an assembly (CATIA product) contain 6 parts.
- Constrain the assembly in such a way that the zero position of the assembly is the same zero position of the D-H coordinate systems.
- Enter the Digital Mockup workbench and create 6 revolute joints.
- Adding 6 formulas to implement the time based kinematics of 6 revolute joints.
- Simulate the robot and generate the 6 revolute joints angles versus time.

The CATIA part design workbench provides operations for creating three-dimensional visual representations of part models. Note that each part models should have a coordinate system attached on it, and the direction and position of these coordinate systems should be the same as the coordinate systems on each links that were chosen by using D-H algorithm. This help to easily verify the solution of simulation model with kinematics of the robot.

The CATIA assembly design workbench provides operation for creating the robot with 6 parts. In this step the kinematics parameters of the assembly should be carefully verified (using Measure tool) and the direction and position of coordinate of each part in assembly product should match exactly with the D-H algorithm coordinate system of each links (using Constraint tool). The CATIA DMU Kinematics workbench allows archive dynamic solutions of the robot simulation. The 6 revolute joints can be created directly by using Kinematics Joints tool or can be automatic assembly constraints conversion by using Assembly Constraints Conversion icon. In order to simulate the mechanism with CATIA, 6 DOFs of mechanism need to be removed by turning all 6 revolute joints into Angle Driven Joints. In this case the lower limit and upper limit are the angle boundary value of each angle joints of robot (from zero position) with the note that the positive/negative rotation should be in the right-handed sense. To get the output solution of mechanism versus time, the velocity of each joints of the robot need to be specified by using Formula icon from the Knowledge toolbar. To get the rotation matrix between the tool frame and the base frame, the angle between each axis of 2 coordinate systems need to be measured by using Measure tool. Since the orientation of the lines is not taken into account, the measured angle values should be carefully checked. The translation vector between tool frame and the base frame of the robot is the coordinate of the origin coordinate system of tool frame that mean the origin of the tool frame should be chosen to archive the translation vector. This can be done by using Speed and Acceleration icon from the DMU Kinematics toolbar. Fig. 4 shows CATIA simulation model with some constraint assembly, 6 revolute joints, 6 Angle driven commands, the fixed part (base frame), 6 formulas, speed and acceleration for the origin of tool frame, and 9 measured angles of rotation matrix between tool frame and base frame.

The excel file solution simulation output can be archived by using Simulation with Laws icon in the Simulation toolbar with the note that the Active Sensor need be checked and chosen the observed sensors. This excel file was used to verify the forward and inverse kinematics and vice versa.

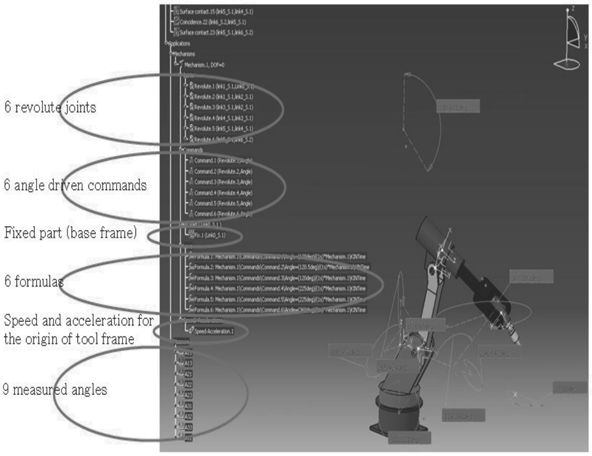

Fig. 4. Catia simulation model of robot

4. Results and discussion

To check the inverse kinematics equations, the rotation matrix of transformation matrix T_0^6 should be carefully measured. Fig. 5 shows the comparison distance results of Catia simulatied and computered kinematics models, in which X, Y, Z are coordinate of origin of tool frame relative to base frame. The compared results, a good agreement between the simulated and calculated models, in each direction X, Y, Z it behaviour the same way with respect to time. Fig. 6 compares the angle of error associated with simulated model and computed inverse kinematic equations at $\Delta\theta_1$ and $\Delta\theta_2$ with respect to time , there is every little difference in error at $\Delta\theta_1$ but at $\Delta\theta_2$ large error difference noted between 0.05-0.15 seconds. The Fig. 7 compares the angle value error between simulated models and computed inverse kinematic equations at $\Delta\theta_3$ and $\Delta\theta_4$, it shows that at $\Delta\theta_4$, the intial rotation there is large error difference of about but as move along with time the angle error is low.

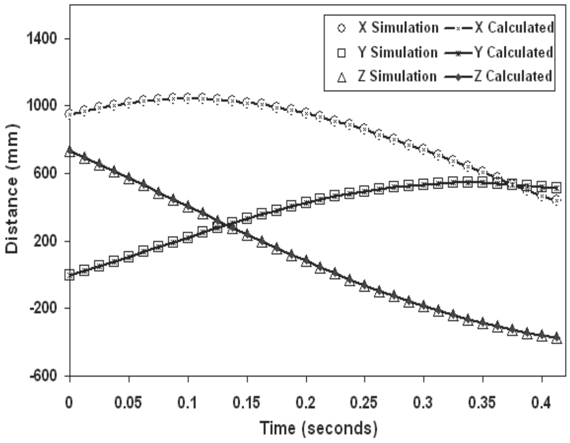

Fig. 5. Comparison distance of simulated model results and calculated results from kinematic equations

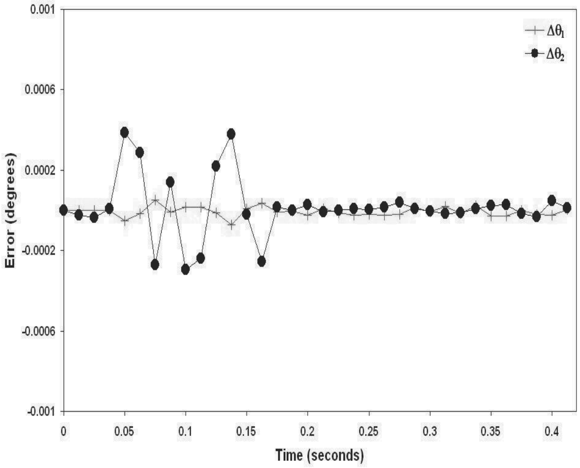

Fig. 6. Comparison angle values error of simulated model results and inverse kinematic equations results for $\Delta\theta_1$ and $\Delta\theta_2$

There is similar error pattern are shown at $\Delta\theta_5$ and $\Delta\theta_6$, where there is very little error at $\Delta\theta_5$ compared to error at $\Delta\theta_6$ as shown in Fig. 8. From the obtained results it is oberved that initial start error associated with simulated model and computed inverse kinematic at $\Delta\theta_1$, $\Delta\theta_3$, $\Delta\theta_5$ is small compared to $\Delta\theta_2$, $\Delta\theta_4$, $\Delta\theta_6$, but as move along with time, all angle value error is almost become zero. According to above results ,the simulations output give good fit to as forward and inverse kinematic results.

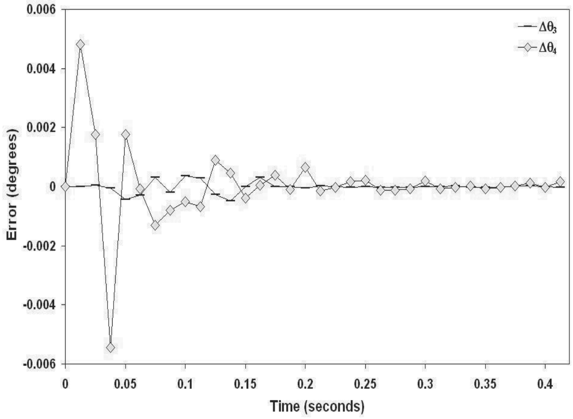

Fig. 7. Comparison angle values error of simulated model results and inverse kinematic equations results for $\Delta\theta_3$ and $\Delta\theta_4$

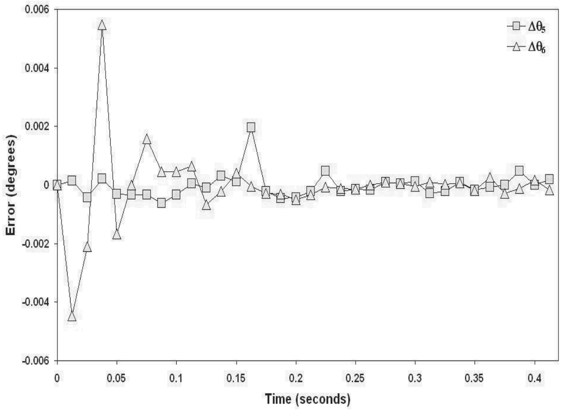

Fig. 8. Comparison angle values error of simulated model results and inverse kinematic equations results for $\Delta\theta_5$ and $\Delta\theta_6$

5. Conclusions

The initial stages for development of welding simulation model has been obtained, the verifying on kinematics make sure that simulation model can be employed for further development. The forward and inverse kinematics of Faraman AM1 welding robot also been provided. The developed Catia Simulation provides good agreement with the forward and inverse kinematics ot the robot. However, in the arc welding process, the kinematics capabilities of a 6-axis industrial robot are not usually sufficient to ensure the required working envelope and/or the desired orientations of the welding torch. Really, it is difficult to simulate the robot moving along the incline weld line with torch angle constraint, that mean the welding system need some more mechanism (for ex. positioner). CATIA V5 software is powerful tool and can be used to develop a simulation welding system.

Acknowledgements

This research was financially supported by the Ministry of Education, Science Technology (MEST) and National Research Foundation of Korea (NRF) through the Human Resource Training Project for Regional Innovation.

References

[1] T.T. Doan, I.S. Kim, H .H. Kim, J.W. Jeong, B.Y. Kang, Developed simulation modal-kinematics for robotics arc welding, Asian International Journal of Scienece and Technology in Production and Manufacturing 1/2 (2008) 69-79.

[2] C.E. Park, J.W. Jeong, A study on the real-time measurement of welding deformation, Journal of Advance Engineering and Technology 2/1 (2009) 199-123.

[3] F.S. Cheng, A methodology for developing robotic workcell simulation models, Proceedings of the 2000 Winter Simulation Conference, Orlando, 2000, 1265-1271.

[4] M. Ericsson, P. Nylén, G. Bolmsjö, Three dimensional simulation of robot path and heat transfer of a TIG-welded part with complex geometry, Proceedings of the 11th International Conference on Computer Technology in Welding, Colorado, 2002, 309-316.

[5] A.P. Pashkevich, A.B. Dolgui, K.I. Semkin, Kinematic aspects of a robot-positioner system in an arc welding application, Control Engineering Practice 11/6 (2003) 633-647.

[6] Jr. Ang, H. Marcelo, W. Lin, S.Y. Lim, A walk-throug programmed robot for welding in shipyards, Industrial Robot 26/5 (1999) 377-388.

[7] P.C. Tung, M.C Wu, Y.R. Hwang, An image-guided mobile robotic welding system for SMAW repair processes, International Journal of Machine Tools and Manufacture 44/11 (2004) 1223-1233.

[8] B.T Lin, S.H. Hsu, Automated design system for drawing dies, Expert Systems with Applications 34/3 (2008) 1586-1598.

[9] W. Skarka, Application of MOKA methodology in generative model creation using CATIA, Engineering Applications of Artificial Intelligence 20/5 (2007) 677-690.

[10] C.H. Chu, M.C. Song, C.S. Luo, Computer aided parametric design for 3D tire mold production, Computers in Industry 57 (2006) 11-25.

[11] T.R. Kurfess (Ed.), Robotics and automation handbook, CRC Press Inc., 2005.

[12] N.G. Zamani, J.M. Weaver, CATIA V5 tutorials, Mechanism design and animation, Release 14 and 15, SDC Publications, Detroid, 2010.

[13] Y. Hurmuzlu, O.D.I. Nwokah, The mechanical systems design handbook, Modeling, measurement and control, CRC Press, 2001.

[14] M. O'Malley, MECH 498, Introduction to robotics, Inverse manipulator kinematics.